Podoplanin is an important stromal prognostic marker in perihilar cholangiocarcinoma

HALMURAT OBULKASIM[*], XIAOLEI SHI[*], JUN WANG, JUN LI, BO DAI,
PENGWEN WU, SHUAI WANG, XUN WANG and YITAO DING

Department of Hepatobiliary Surgery, The Affiliated Drum Tower Hospital of Nanjing
University Medical School, Nanjing, Jiangsu 210008, P.R. China

Abstract. Cancer-associated fibroblasts (CAFs) exhibit various phenotypes and serve an important role in tumor progression. However, research on podoplanin expression in CAFs is limited, and its role in the cholangiocarcinoma microenvironment remains unclear. The present study analyzed the clinical and pathological records of 42 patients diagnosed with perihilar cholangiocarcinoma (pCCA) in The Affiliated Drum Tower Hospital of Nanjing University Medical School (Nanjing, China). Immunohistochemical staining was performed to evaluate the expression of podoplanin in CAFs in order to determine its association with clinicopathological parameters and survival rate. Podoplanin expression in the CAFs was associated with the tumor-node-metastasis staging system, and lymph node metastasis in pCCA. Tumor tissue demonstrated an increase in lymphatic vessel density (LVD) compared with para-tumor tissue. Podoplanin expression in CAFs was associated with LVD in tumor and para-tumor tissues. To examine the effect of podoplanin expression in CAFs on tumor progression, CAFs were isolated from tumor xenografts. Following transfection with an expression plasmid encoding podoplanin, the migratory ability of CAFs was significantly increased. Therefore, CAF-associated podoplanin expression in pCCA may serve as a potential biomarker to evaluate prognosis and provide a valuable target for anticancer therapy.

Correspondence to: Professor Yitao Ding, Department of Hepatobiliary Surgery, The Affiliated Drum Tower Hospital of Nanjing University Medical School, 321 Zhongshan Road, Nanjing, Jiangsu 210008, P.R. China
E-mail: yitaodingdrumtower@126.com

[*]Contributed equally

Introduction

Cholangiocarcinoma (CCA) is a malignant tumor originating from biliary epithelial cells. In total, >50% of CCAs are referred to as perihilar CCAs (pCCAs) or Klatskin tumors. pCCAs occur at the junction between the cystic duct and common/second degree bile ducts (1). Tumor invasion and lymph node metastasis are the primary factors, which need to be considered prior to pCCA treatment as this may affect overall prognosis and treatment options (2). Surgical resection is considered the preferred option for pCCA treatment; however, it is difficult to perform and often ineffective, which may explain the increasing mortality rates observed worldwide (3). Therefore, it is important to research and identify more effective molecular targets for pCCA therapy.

pCCA is highly desmoplastic in nature, and is surrounded by a large amount of stroma containing several activated myofibroblasts termed cancer-associated fibroblasts (CAFs) (4). Vimentin, fibroblast-specific protein 1 (FSP1) and α-smooth muscle actin (α-SMA) are collectively considered as specific biomarkers for CAFs (5). CAFs affect the biological behavior (s) of tumors, including tumor proliferation, invasion and metastasis. During cancer progression, invasive cancer cells are able to pass through the basement membrane into the vascular or lymphatic system (6). Lymphatic vessel density (LVD), which is defined by the number of lymphatic vessels in a given area, may contribute to lymph node metastasis and increase the possibility of invasion (7). In the present study, clinical data revealed that the expression of podoplanin in CAFs was associated with lymph node metastasis. Lymphangiogenesis serves a crucial role in tumor progression as it may promote metastasis (8). Several previous studies also reported the association between LVD and lymph node metastasis, and the associated unfavorable overall prognosis (9,10). Therefore, the expression of podoplanin in CAFs, and its significance in lymphangiogenesis requires further investigation.

Podoplanin, a 38 kDa type I transmembrane glycoprotein, is expressed in several types of malignant tumor cells, including epithelial cells and CAFs (11-15). Cell migration and invasion are initiated by the protrusion of the cell membrane, which is physically mediated by the actin cytoskeleton (16). A previous study demonstrated that podoplanin is present in extracellular and intracellular regions (17). Furthermore, its intracellular

binding with ezrin, radixin and moesin (ERM) proteins is considered to lead to morphological changes and cytoskeletal reorganization in cells (18). Cofilin-1 is an important actin-binding protein, and is able to modulate the cytoskeleton that affects actin polymerization, generation of protrusions and the direction of cell migration (19). Maintenance and functional activity of CAFs is dependent on a high level of actomyosin contractility. Actomyosin contractility, which may lead to matrix remodeling, is generated by phosphorylation of myosin light-chain 2 (MLC-2) (20). It is hypothesized that podoplanin expression in CAFs may influence actomyosin contractility and modulation of the cytoskeleton in order to enhance the migration ability of CAFs.

In the present study, CAF podoplanin expression levels in 42 patients with pCCA were analyzed, and the effect of podoplanin-positive CAFs in pCCA progression is discussed.

Materials and methods

Patients and tissue samples. Paired paraffin-embedded tumor and para-tumor tissues were obtained from the Department of Pathology of The Affiliated Drum Tower Hospital of Nanjing University Medical School (Nanjing, China) with the approval of the Ethics Committee of the Nanjing Drum Tower Hospital (Nanjing, China). A total of 42 samples from patients with pCCA who also underwent surgical resection between September 2000 and December 2012 were analyzed. Para-tumor tissue was confined to tissue that was ~2 cm from the tumor margin. Clinicopathological details of patients and tumors were retrieved from medical records and are presented in Table I.

Hematoxylin and eosin (H&E) staining, and immunohistochemical (IHC) evaluation. Tissues were fixed in 10% buffered formalin for 8 h at 4˚C and embedded in paraffin at room temperature. Sections were cut (5 μm thick) for H&E staining and IHC evaluation. All sections were deparaffinized and rehydrated with serial dilutions of ethanol. Tissue sections were immunostained with primary antibodies against α-SMA (mouse anti-human monoclonal antibody; 1:500; cat. no. ab119952; Abcam, Cambridge, MA, USA), vimentin (rabbit monoclonal antibody; 1:900; cat. no. ab92547; Abcam) and podoplanin (rabbit polyclonal anti-human; 1:500; cat. no. sc-134482; Santa Cruz Biotechnology, Inc., Dallas, TX, USA) overnight at 4˚C. The following day, sections were incubated with goat anti-rabbit immunoglobulin G (IgG) secondary antibody (cat. no. TA130015; 0.5 μg/ml; OriGene Technologies, Inc., Beijing, China) or goat anti-mouse IgG secondary antibody (cat. no. TA130070; 0.5 μg/ml; OriGene Technologies, Inc., Beijing, China) at 37˚C for 30 min. Sections were then stained with 3,3'-diaminobenzidine and counterstained with hematoxylin. A distribution score that reflected the distribution of positive signals among stromal cells was determined as 0 (0%), 1 (1-50%) or 2 (5-100%). Scores reflected the percentage of positive staining of stromal cells within the same tissue section. The signal intensity score was evaluated as 0 (no signal or weak), 1 (moderate) or 2 (strong) in accordance with the method of Fukuoka *et al* (21). The sum of the distribution and intensity scores (range, 0-4) was used as a total score (TS): 0 (sum, 0), 1 (sum, 1), 2 (sum, 2) and 3 (sum,

3 or 4). A TS of 0 and 1 was considered negative, whereas a TS of 2 and 3 was considered positive. In the situation where there was a discrepancy in scores between duplicated cores from the same patient, the higher score was assigned as the final score. Quantitative analysis of lymphatic vessels was also performed, with podoplanin-labeled lymphatic endothelial cells with brownish yellow staining considered a positive standard. Three optical fields with the most vascularized areas were selected at low magnification (x40) for each sample using a light microscope (Olympus Corporation, Tokyo, Japan). Lymphatic vessels were counted at high magnification (x200). LVD was analyzed according to a protocol described in a previous study (22).

Cell culture. CCA cell line QBC939 was purchased from the Cell Bank of the Chinese Academy of Sciences (Shanghai, China). Human dermal lymphatic endothelial cells (HDLECs) were purchased from Scien Cell Research Laboratories (Carlsbad, CA, USA). QBC939 cells were cultured in RPMI-1640 medium with 10% fetal bovine serum (FBS; Gibco; Thermo Fisher Scientific, Inc., Waltham, MA, USA) and 1% penicillin/streptomycin. HDLECs were cultured in endothelial cell medium with 1% endothelial cell growth supplement, 5% FBS and 1% penicillin/streptomycin. HDLECs which were passaged between 2 and 7 times were used for later experiments. Cells were grown at 37˚C in a humidified incubator with 5% CO_2.

Isolation of CAFs from CCA tumor xenograft. Pathogen-free BALB/C nude mice (n=5) aged 4-5 weeks (weight, 20 g; male) were obtained from the Animal Center of Nanjing Drum Tower Hospital (Nanjing, China). The National Research Council Guide for the Care and Use of Laboratory Animals (23) was followed (12-h light/12-h dark cycle; temperature, 24˚C; humidity, 65%) and ethical approval was obtained from the Ethics Committee of The Nanjing Drum Tower Hospital. The mice were allowed free access to food and water. QBC939 CCA cells were injected subcutaneously into the right flanks of the mice (10^6 cells/mouse). After 4 weeks, all mice were sacrificed and the xenograft tumors were harvested. Tumor tissues were cut into small fragments, placed in digestion solution of 0.1% type IV collagenase (Sigma-Aldrich; Merck KGaA, Darmstadt, Germany) with 10% FBS (Gibco; Thermo Fisher Scientific, Inc.) and incubated at 37˚C in a humidified 5% CO_2 incubator for 6 h. Cells were separated from the digested tissue and filtered through a 70 μm cell strainer. Following centrifugation (at 700 x g for 5 min at 20˚C), adherent cells were collected and CAFs were purified by repeated brief exposure (within 3 min) to 0.25% trypsin-EDTA (Gibco; Thermo Fisher Scientific, Inc.), also termed differential trypsinization. The medium was changed after 30 min (differential adhesion) (24). CAFs were grown at 37˚C in a humidified 5% CO_2 forced-air incubator.

Adenovirus transfection. CAFs were seeded at $5x10^4$ cells/well into 24-well plates for 24 h, and then transfected with adenovirus containing either the podoplanin gene (Ad-podoplanin) or no podoplanin gene (Ad-vector) at a multiplicity of infection of 50. The culture medium was replaced with fresh medium 8 h later, and cells were cultured overnight. The expression

levels of podoplanin protein were determined using western blotting.

Dual immunofluorescence staining. Frozen tissue sections were fixed in acetone for 20 min at 4°C and blocked with 5% bovine serum albumin/PBS for 1 h and incubated with anti-α-SMA antibody (mouse anti-human monoclonal; 1:500; cat. no. ab119952; Abcam) and anti-podoplanin antibody (rabbit anti-human; polyclonal 1:200; cat. no. sc-134482; Santa Cruz Biotechnology, Inc.) overnight at 4°C. Secondary antibodies including Alexa Fluor 488-conjugated goat anti-mouse IgG (1:500; cat. no. ab150113; Abcam) and cyanine (Cy) 3-conjugated goat anti-rabbit IgG (1:2,000; cat. ab970075; Abcam) were applied for 1 h, and counterstained with DAPI (Merck KGaA), and washed three times with PBS. The same protocol was used for dual immunofluorescence staining of cultured CAFs grown in chamber slides. Slides were reacted with anti-α-SMA monoclonal antibody (mouse anti-human; monoclonal; 1:500; cat. no. ab119952; Abcam), rabbit anti-FSP1 polyclonal antibody (1:100; cat. no. ab27957; Abcam) and rabbit anti-vimentin monoclonal antibody (1:1,000; cat. no. ab92547; Abcam) overnight at 4°C. This was followed by incubation with Alexa Fluor 488-conjugated goat anti-mouse IgG (1:500; cat. no. ab150113; Abcam) and Cy3-conjugated goat anti-rabbit IgG (1:1,000; cat. no. ab97075; Abcam) for 1 h, and counterstained with DAPI (Merck KGaA). Once slides were mounted with mounting medium (cat. no. ab128982; Abcam), slides were examined using laser-scanning confocal microscopy.

Flow cytometry. Isolated CAFs were trypsinized and centrifuged at 200 x g for 5 min, fixed with 80% methanol for 5 min and permeabilized with 0.1% PBS/Triton X-100 for 15 min. Following washing twice with PBS, cells were incubated with antibodies against vimentin (rabbit monoclonal anti-human; 1:50; cat. no. ab92547; Abcam), α-SMA (mouse monoclonal anti-human; 1:200; cat. no. ab119952; Abcam) and anti-FSP1 (rabbit polyclonal anti-human; 1:100; cat. no. ab27957; Abcam) for 1 h at room temperature. Following incubation, Alexa Fluor 488-conjugated goat anti-mouse IgG (1:250; cat. no. ab150113; Abcam) and Cy3-conjugated goat anti-rabbit IgG (1:500; cat. no. ab97075; Abcam) were applied for 30 min at room temperature. Anti-mouse podoplanin (1:100; cat. no. 12-5381; BD Biosciences, San Jose, CA, USA) was used for the detection of podoplanin-positive cells. Flow cytometry data were analyzed using FlowJo software (version 7.6; FlowJo LLC, Ashland, OR, USA).

Western blotting. The tissue was homogenized in radioimmunoprecipitation assay lysis buffer (cat. no. P0013B; Beyotime Biotechnology, Shanghai, China) and incubated on ice for 30 min. The supernatant following centrifugation (at 15,000 x g for 15 min at 4°C) was used for western blotting. Western blotting was performed as described previously (25). Blots were incubated overnight with the following primary antibodies: Anti-podoplanin (rabbit polyclonal antibody; 1:300; cat. no. 251419; Abbiotec, San Diego, CA, USA), anti-β-tubulin (mouse monoclonal antibody; 1:5,000; cat. no. AT0003; CMCTAG, Inc., Milwaukee, WI, USA) and anti-cofilin (rabbit monoclonal antibody; 1:1,000; cat. no. 5175, Cell Signaling Technology, Danvers, MA, USA), anti-phospho-cofilin (rabbit

monoclonal antibody; 1:1,000; cat. no. 3313; Cell Signaling Technology), anti-ERM (rabbit monoclonal antibody; 1:1,000; cat. no. 3142; Cell Signaling Technology), anti-phospho-ERM (rabbit monoclonal antibody; 1:1,000; cat. no. 3726; Cell Signaling Technology), anti-MLC-2 (rabbit monoclonal antibody; 1:1,000; cat. no. 8505; Cell Signaling Technology) and anti-phospho-MLC-2 (1:1,000; cat. no. 3671; Cell Signaling Technology). Western blots were visualized using an electrophoretic gel imaging system (Shanghai, China).

Migration assay. Cell migration was determined using a modified two-chamber migration assay (Corning Incorporated, Corning, NY, USA) with a pore size of 8 μm. Cells (Ad-podoplanin CAFs and Ad-vector CAFs) were seeded in 1% FBS/Dulbecco's modified Eagle's medium (DMEM) in the upper chamber at a concentration of $2x10^5$ cells/ml, and the lower chamber was filled with 10% FBS/DMEM. After 24 h of incubation at 37°C, cells within the upper chamber were removed with a cotton swab. Cells which had migrated across the membrane were fixed in 4% paraformaldehyde at 37°C for 30 min, stained with crystal violet (0.5% in 20% methanol) at room temperature for 30 min. Stained cells were counted in five randomly selected fields using a light microscope (magnification, x100; Olympus Corporation).

HDLEC tube-formation assay. Matrigel matrix (BD Biosciences) was added to 96-well plates (50 μl to each chamber) and allowed to polymerize for 30 min at 37°C. HDLECs were diluted with the supernatant of Ad-podoplanin CAFs and Ad-vector CAFs at $5x10^4$ cells/ml. For the vector group, 10% FBS medium was used. Tube formation was observed after 6 h.

Statistical analysis. Results are presented as the mean ± standard deviation. Comparisons between two groups were made using Student's t-test. A χ^2 test was used to analyze associations between immunohistochemistry staining of podoplanin in CAFs, and clinicopathological characteristics. Survival curves were constructed using the Kaplan-Meier estimator curves method and compared using a log-rank test. All statistical analyses were performed using SPSS (version 22; IBM Corp., Armonk, NY, USA) software and GraphPad Prism (version 5; GraphPad Software, Inc., La Jolla, CA, USA). $P<0.05$ was considered to indicate a statistically significant difference.

Results

Observation of CAFs in the pCCA tumor microenvironment. Immunofluorescence staining of patient samples demonstrated numerous spindle-shaped stromal cells stained with α-SMA, which were recognized as CAFs (Fig. 1A). A portion of the CCA epithelium was also positive for α-SMA. Dual immunolabeling indicated that certain CAFs in the tumor microenvironment were podoplanin-negative, whereas others were podoplanin-positive (Fig. 1B). In addition, certain epithelial cells were positive for podoplanin. Therefore, podoplanin expression in the CAFs may serve a role in pCCA development.

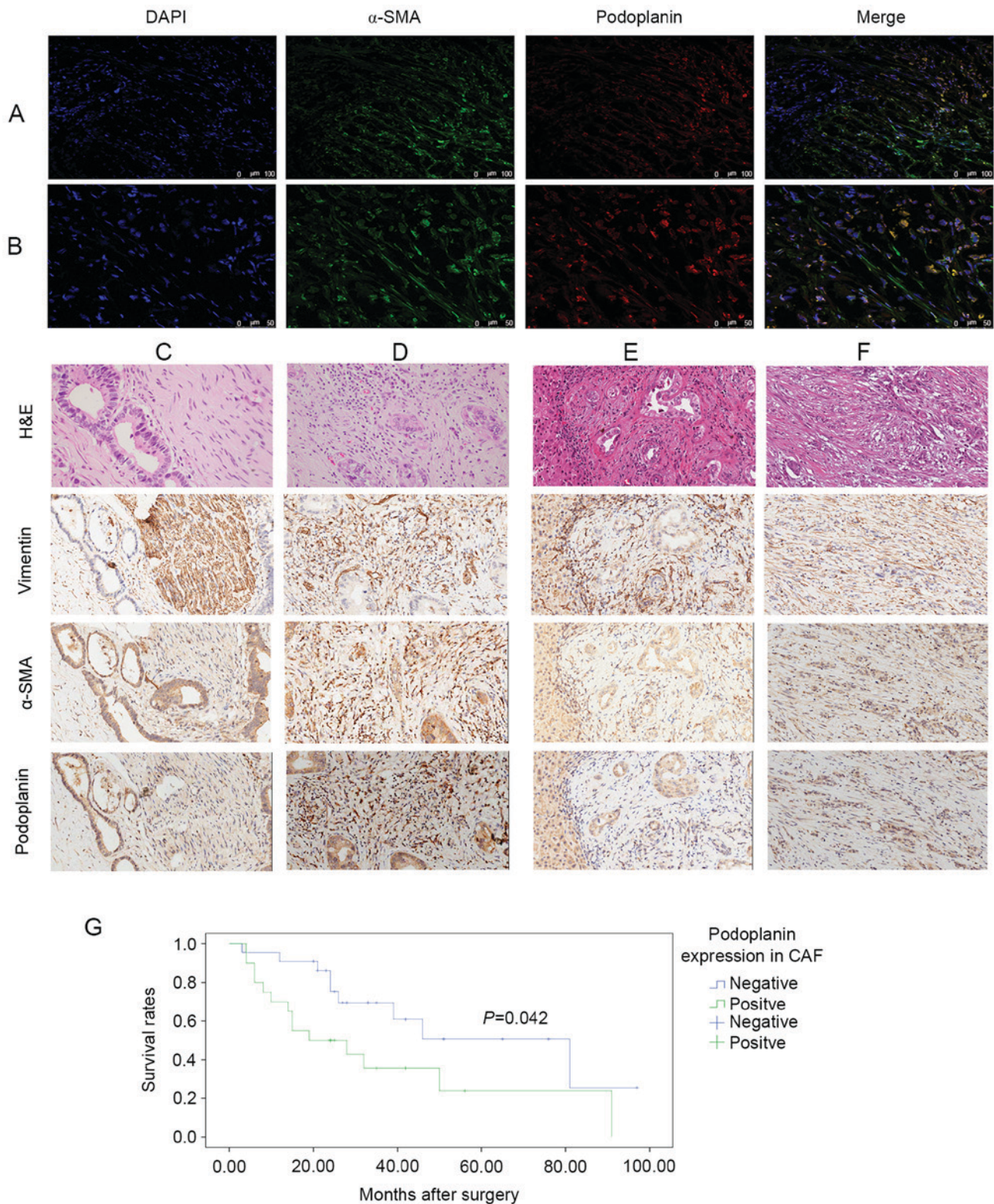*Association between podoplanin expression in CAFs and pathological parameters.* Podoplanin expression levels in

Figure 1. Podoplanin expression levels in CAFs. Multicolor images of immunofluorescence labeling for α-SMA (fluorescein isothiocyanate; FITC) and podoplanin (Cy3). Nuclear staining with DAPI demonstrated that podoplanin-negative and podoplanin-positive CAFs are present in pCCA. Original magnification (A) x200, (B) x400. H&E and IHC staining were performed on pCCA and para-tumor sections. Four sections were stained with H&E, and α-SMA, vimentin and podoplanin were immunolabeled in each group. H&E, vimentin and α-SMA were used for CAF recognition. Magnification x200. Representative (C) podoplanin-negative and (D) podoplanin-positive CAFs in tumor tissue. Representative (E) podoplanin-negative and (F) podoplanin-positive CAFs in para-tumor tissue. (G) Kaplan-Meier estimator curves demonstrating overall survival for 42 patients with pCCA; a significant difference in cumulative overall survival was observed between patients who were positive or negative for podoplanin expression in CAFs. (P=0.042, log-rank test). CAF, cancer-associated fibroblast; Cy, cyanine; pCCA, perihilar cholangiocarcinoma; H&E, hematoxylin and eosin; α-SMA, α-smooth muscle actin.

pCCA tumor tissue was observed in lymphatic vessel endothelium, tumor epithelium and tumor stroma. CAFs were the primary component of the tumor microenvironment, and stromal podoplanin was expressed primarily within these

cells. CAFs were identified as large spindle-shaped cells using H&E and IHC staining. Stroma were identified through H&E staining and by cell shape, and IHC staining for α-SMA and vimentin was used to confirm the presence of CAFs. Expression levels of podoplanin in pCCA tumor (Fig. 1C and D) and para-tumor (Fig. 1E and F) tissues were investigated. The proportion of podoplanin-positive CAFs in the para-tumor tissue was decreased and the cells exhibited less marked staining compared with in the tumor tissue. The ratio of podoplanin-positive CAFs to podoplanin-negative CAFs in the para-tumor tissue was 8:42, and all podoplanin-positive CAFs were stained weakly to moderately. In comparison, the ratio of podoplanin-positive CAFs in tumor tissue was 20:42, and stained strongly. In addition, podoplanin expression levels in CAFs significantly differed between paired tumor and para-tumor tissues (P<0.05).

The clinicopathological characteristics of 42 patients with pCCA and their association with podoplanin expression levels in CAFs are summarized in Table I. Out of the 42 specimens, 20 had podoplanin-positive CAFs in the tumor tissue. Compared with the podoplanin-negative CAF group, the podoplanin-positive CAF group was significantly associated with lymph node metastasis and tumor-node-metastasis (TNM) staging. Survival analysis indicated that the median survival time was 31.59 months, and the 1-, 3- and 5-year survival rates were 90, 66 and 53% in the podoplanin-negative CAF groups, and 57, 37 and 26% in the podoplanin-positive CAF groups. The overall survival rate in the podoplanin-negative CAF group were significantly increased compared with the podoplanin-positive CAF group (P=0.042, log-rank test, Fig. 1G). This indicated that podoplanin-positive CAFs in the tumor microenvironment may lead to more frequent lymph node metastases and promote tumor progression.

Association between lymphatic vessel density and podoplanin expression levels in CAFs. A total of 42 paired tumor and para-tumor samples were used to count lymphatic vessels (Fig. 2), which were visualized using IHC staining (Fig. 2A and B). Results demonstrated an increase in the number of lymphatic vessels in the tumor tissue compared with the para-tumor tissue (Fig. 2E). Tumor tissue from patients with podoplanin-positive CAFs (Fig. 2C) exhibited increased LVD compared with patients with podoplanin-negative CAFs (Fig. 2D). There were significant differences between LVD and podoplanin expression levels in CAFs of tumor and para-tumor tissue (Fig. 2F).

Podoplanin overexpression in CAFs enhances migration ability and does not affect tube formation. In podoplanin-positive CAFs, there was a significant association between TNM stage and lymph node metastasis. Quantification of the association between LVD in the tumor and para-tumor tissue, the presence of podoplanin-positive CAFs and the occurrence of lymph node metastasis indicated that podoplanin may serve an important role in tumorigenesis and metastasis. To test this hypothesis, CAFs were isolated from pCCA tumor xenografts in the present study. Characterization of cells using dual immunofluorescence staining (Fig. 3A and B) with antibodies against α-SMA, vimentin and FSP1 were performed. Analysis of the proportion of CAFs using double-staining flow cytometry was also performed. Results demonstrated that 97.6% of purified CAFs

Table I. Associations between podoplanin expression in cancer-associated fibroblasts and clinicopathological characteristics of perihilar cholangiocarcinoma.

Parameter	n	Tumor tissue		P-value
		Positive	Negative	
Sex				0.051
Male	25	15	10	
Female	17	5	12	
Age, years				0.067
≤55	19	12	7	
>55	23	8	15	
Tumor size, cm				0.536
<3	21	11	10	
≥3	21	9	12	
Differentiation				0.871
Well (G1)-moderate (G2)	33	16	17	
Poor (G3)	9	4	5	
TNM stage				0.002[a]
I+II	21	5	16	
III+IV	21	15	6	
Chronic cholangitis				0.406
Yes	30	16	14	
No	12	4	8	
Neural invasion				0.489
Positive	35	18	17	
Negative	7	2	5	
Vascular invasion				0.569
Positive	17	9	8	
Negative	25	11	14	
Cancer embolus				0.126
Positive	14	9	5	
Negative	28	11	17	
Lymph node metastasis				0.014[a]
Present	19	13	6	
Absent	23	7	16	

[a]P<0.005. TNM, tumor-node-metastasis.

were positive for α-SMA and vimentin (Fig. 3C), and 93.2% of these CAFs were positive for FSP1 (Fig. 3D). In addition, flow cytometry results demonstrated that 11% of these CAFs were positive for podoplanin (Fig. 3E). To understand the function of podoplanin in the CAFs, CAFs were transfected with Ad-podoplanin adenovirus and examined using western blotting (Fig. 4A). Determination of whether podoplanin overexpression affected the migration ability of CAFs was performed (Fig. 4B), and the number of Ad-podoplanin CAFs which passed through the membrane into the lower chamber was significantly increased compared with the Ad-vector CAFs (P<0.01). Additionally, ERM, MLC and cofilin were phosphorylated in Ad-podoplanin CAFs (Fig. 4A). The results indicate that podoplanin has an important function in CAF migration.
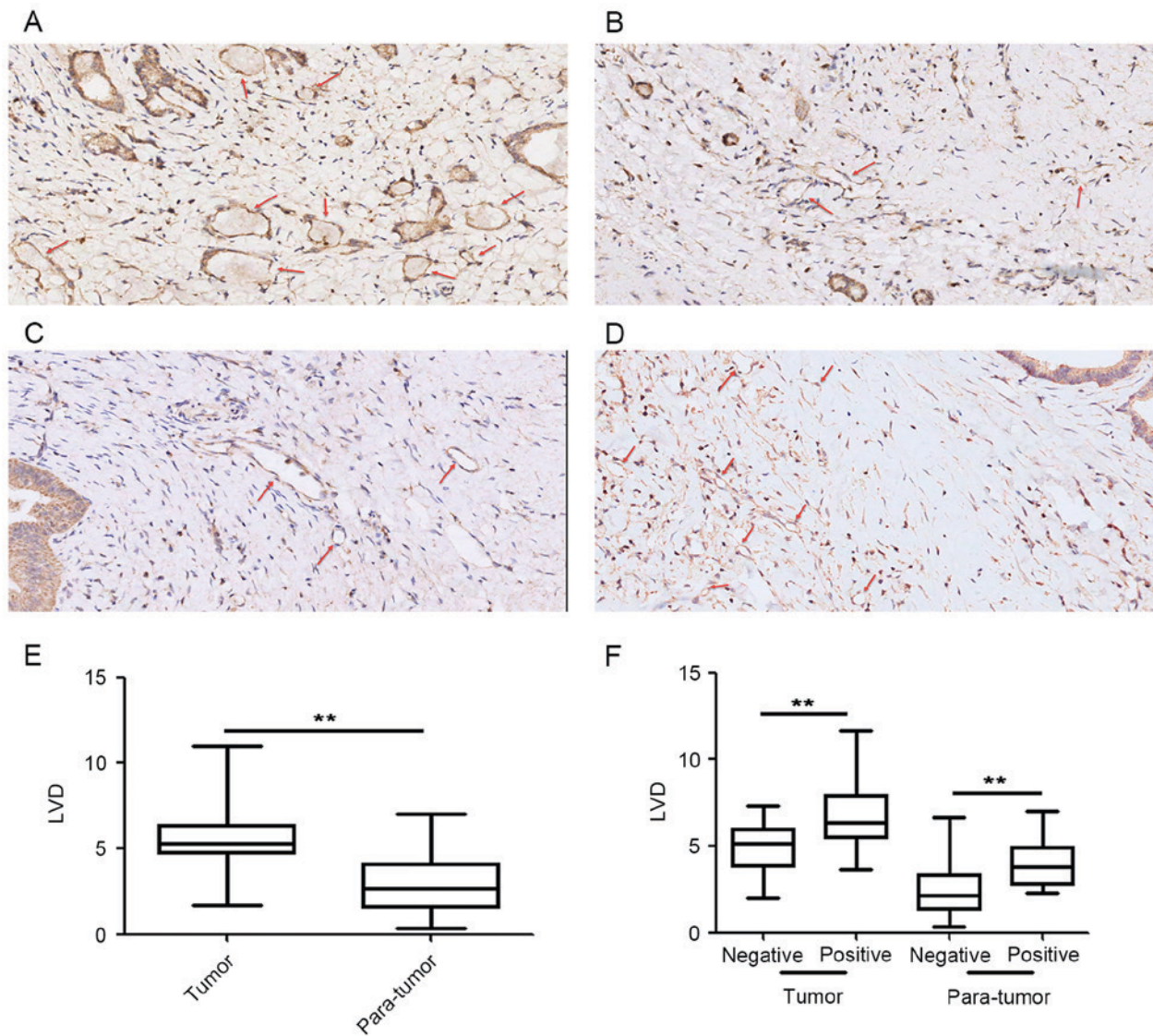
Figure 2. Association between podoplanin expression levels in CAFs and LVD in pCCA. Lymphatic vessels (red arrows) stained using immunohistochemistry with anti-podoplanin antibody in (A) tumor and (B) para-tumor tissue. Magnification, x200. Red arrows indicate lymphatic vessels in tumor tissue with (C) podoplanin-negative CAFs and (D) podoplanin-positive CAFs. Magnification, x200. (E) Box-plot demonstrating the mean LVD in tumor and para-tumor tissue (P<0.01). (F) Significant association between the mean LVD and podoplanin expression levels in CAFs in tumor (P<0.01) and para-tumor tissue (P<0.01). **P<0.01. CAF, cancer-associated fibroblasts; LVD, lymphatic vessel density; pCCA, perihilar cholangiocarcinoma.

The effects of transfection with the podoplanin expression vector and control vector on CAF tube formation are presented in Fig. 4C. Podoplanin overexpression in CAFs did not significantly affect the tube-formation ability of lymphatic endothelial cells. Therefore, overexpression of podoplanin in CAFs may enhance migration and adhesion; however, it does not directly influence tube formation in lymphatic endothelial cells.

Discussion

Cholangiocytes possess different morphologies and phenotypes at various anatomical levels of the biliary tract; these differences may reflect various clinicopathological features of CCA (26). Patients with pCCA exhibit an increase in lymph node metastasis rate compared with patients with hepatocellular carcinoma. Lymph node metastasis is an important prognostic factor for the survival rate of patients

with pCCA following resection (27,28). Therefore, it may be of importance to study the lymphatic system in pCCA further.

Podoplanin has emerged as a potential therapeutic target in tumor cells (29). Previous research has primarily focused on the tumor microenvironment, which may have a major impact on the progression and dissemination of tumor cells (30). In particular, CAFs, which are the primary constituent of the tumor microenvironment, are able to affect tumor epithelial cells and other cell types through secretion of cytokines and growth factors (31). Results from the present study demonstrated that podoplanin was expressed in a group of CAFs and epithelial tumor cells in pCCA specimens, and demonstrated that several clinicopathological characteristics, including TNM stage and lymph node metastasis, were associated with podoplanin expression. Survival analysis also demonstrated that increased expression levels of podoplanin in CAFs were associated with poor patient outcome. Previous
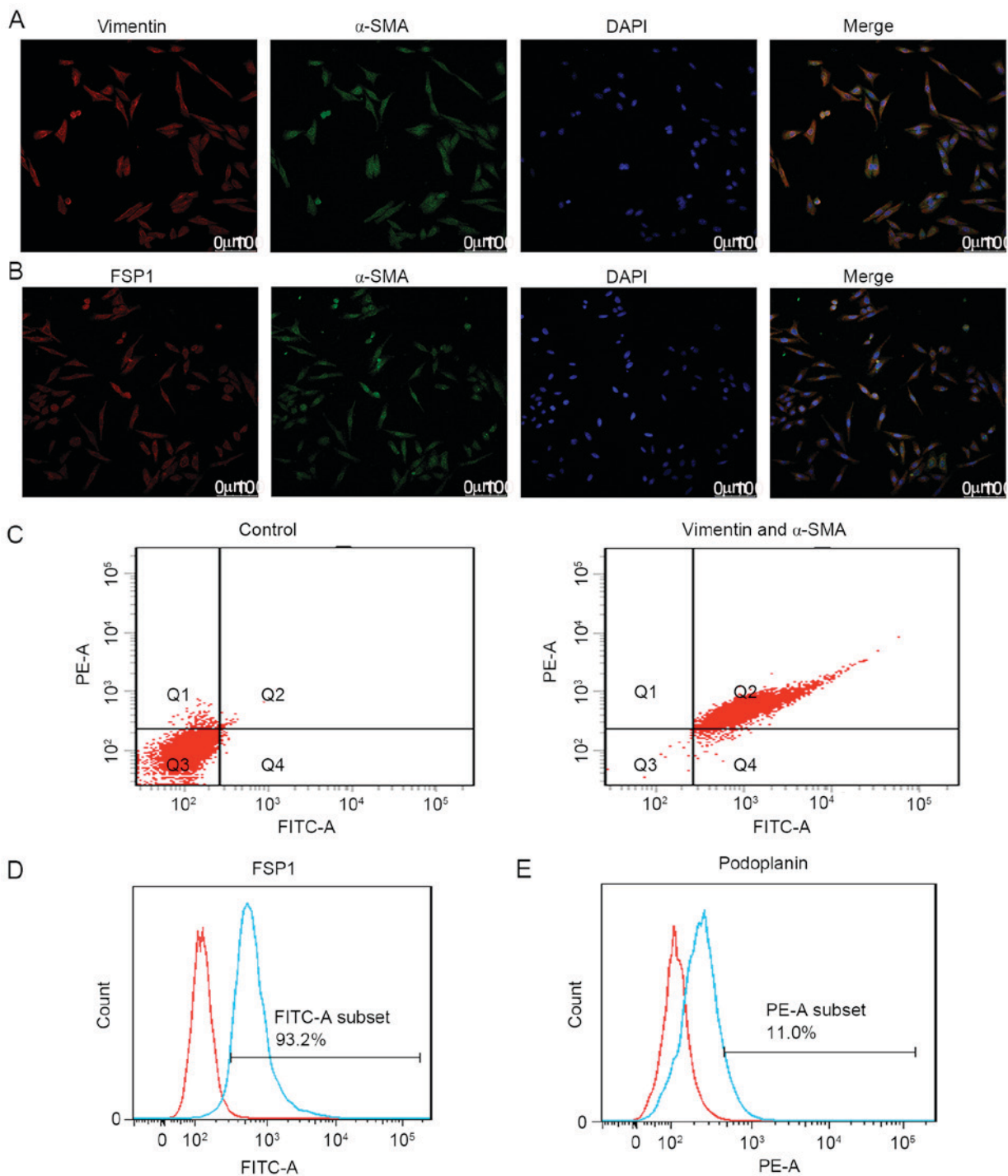
Figure 3. Immunofluorescence and flow cytometry for the identification of CAFs and their phenotype. (A) Representative images of dual immunofluorescence staining of cultured CAFs with α-SMA (green) and vimentin (red) antibodies. (B) Representative images of dual immunofluorescence staining of cultured CAFs with anti-α-SMA (green) and anti-FSP1 (red) antibodies; all groups were counterstained with DAPI (blue); magnification, x200. Representative flow cytometry results for CAFs; cells expressed (C) vimentin and α-SMA, and (D) FSP1. Cells positive for vimentin (PE) and α-SMA (FITC) accounted for 97.6% of the CAF population. FSP1-positive cells (FITC) accounted for 93.2% of the CAF population. (E) Podoplanin-positive cells (PE) accounted for 11% of the CAF population. CAF, cancer-associated fibroblast; α-SMA, α-smooth muscle actin; FSP1, fibroblast-specific protein 1; FITC, fluorescein isothiocyanate, PE, phycoerythrin.

studies have reported high podoplanin expression in several squamous cell carcinomas, including esophageal, oral and lung carcinomas, which were associated with a decreased survival rate and an increased incidence of lymph node metastasis (12,17,32,33). However, in certain types of cancer, such as squamous non-small cell lung cancer and colorectal carcinoma, increased levels of podoplanin expression is associated with a favorable prognosis. Therefore, podoplanin serves as a good prognostic marker for different types of tumor or tumors presenting at different stages.

Tumor metastasis is a complex and multistep process. First, tumor cells separate from the primary tumor mass, and then degrade and penetrate the extracellular matrix and enter the bloodstream or lymphatic system. Following activation in
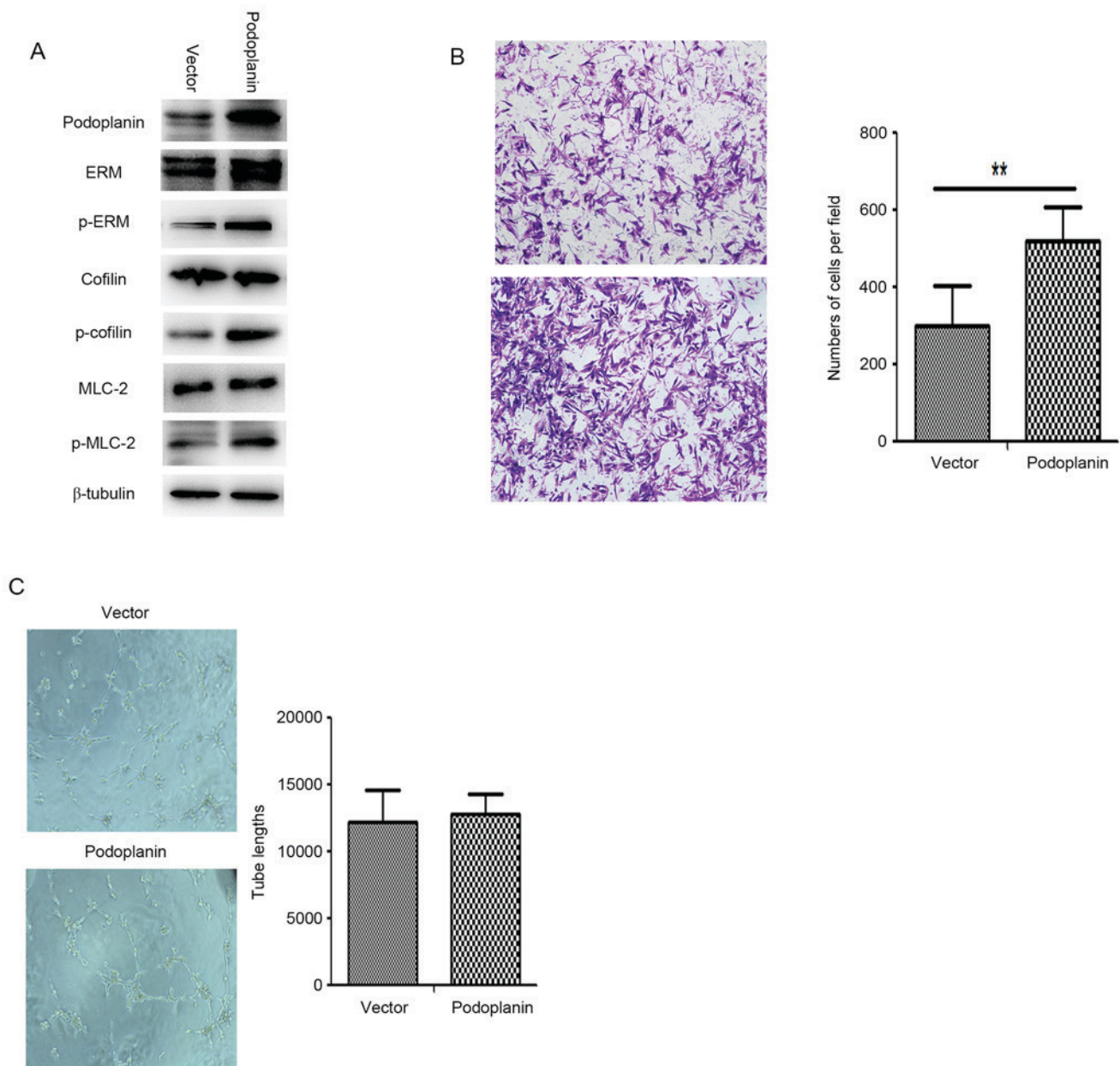
Figure 4. Podoplanin overexpression enhances the migration ability of CAFs. (A) Following transfection of CAFs with a podoplanin plasmid, western blotting demonstrated significant phosphorylation of ERM, cofilin and MLC compared with the vector group. (B) Cells were stained with crystal violet and observed using light microscopy (magnification, x100). Transwell migration assays demonstrated differences in migratory cells between podoplanin-positive and podoplanin-negative CAFs ($P<0.01$). (C) Conditioned medium from podoplanin-positive CAFs had no influence on tube formation in HDLECs. Representative pictures of tube formation are exhibited. Quantitative analysis of the lack of tube formation by HDLECs induced by conditioned medium; mean ± standard deviation; no significant differences were demonstrated (n=5). In (B) and (C), all data are representative of three independent experiments. **$P<0.01$. p-, phosphorylated; ERM, ezrin, radixin and moesin; MLC-2, myosin light chain 2; CAF, cancer-associated fibroblast; HDLEC, human dermal lymphatic endothelial cell.

the tumor microenvironment, CAFs may facilitate invasion and migration of cancer cells by remodeling the extracellular matrix (34). The results of the present study demonstrated that podoplanin overexpression significantly increased the migration ability of CAFs. Western blotting indicated that phosphorylation of ERM, MLC-2 and cofilin was upregulated in podoplanin-overexpressing CAFs. Previous studies have reported that podoplanin regulates Rho activity in lymphatic endothelial and fibroblastic reticular cells (35,36). In addition, podoplanin is able to affect the cytoskeleton by binding and activating members of the ERM family. Cofilin is an actin-remodeling protein that is able to generate significant differences in migration, invasion and metastatic potential in human cancer cells (37). MLC is the key regulator of actin-myosin contractility. Phosphorylation of cofilin and MLC-mediated remodeling of the actin network serve important roles in cancer cell migration and invasion (38). Results demonstrated that podoplanin overexpression in CAFs enhances migration ability by regulating the actin network.

Ochoa-Alvarez *et al* (39) demonstrated that a podoplanin-expressing tumor xenograft established using a human oral cancer cell line was able to induce podoplanin expression in infiltrating mouse CAFs. In the present study, isolation of CAFs from a CCA tumor xenograft identified that 11% of these CAFs expressed podoplanin using flow cytometry analysis. Podoplanin expression in tumor xenograft stromal cells may depend on the human oral cancer cell line and tumorigenesis time following injection. Tumor xenograft models have been widely used in pharmacokinetic and bioavailability studies. Yoshida *et al* (40) reported that podoplanin-positive CAFs served an important role in primary resistance to epidermal growth factor receptor tyrosine kinase inhibitors. Previous studies also reported that podoplanin-mediated epithelial-mesenchymal transition (EMT) may contribute to tumor epithelial cell invasion (17,41). EMT is considered a dispensable pathway for metastasis; however, recently it has also been demonstrated to contribute to chemoresistance (42). These results collectively suggest that the effect of chemotherapy may depend on cancer cells and the surrounding tumor microenvironment. The mechanism of podoplanin-mediated EMT and the association between podoplanin expression in CAFs, and chemoresistance in the tumor microenvironment are not fully understood. Further elucidation of how podoplanin affects tumor migration, invasion and chemoresistance in CCA will be essential to develop means to limit excessive podoplanin expression in CAFs, and inhibit the podoplanin-mediated signaling pathways in CCA; this may offer new therapeutic strategies for treating pCCA. Further investigation into accurate prognostic information regarding pCCA is required.

Acknowledgements

References

1. Razumilava N and Gores GJ: Cholangiocarcinoma. Lancet 383: 2168-2179, 2014.
2. Zeng X and Tao H: Diagnostic and prognostic serum marker of cholangiocarcinoma (Review). Oncol Lett 9: 3-8, 2015.
3. Rizvi S and Gores GJ: Pathogenesis, diagnosis, and management of cholangiocarcinoma. Gastroenterology 145: 1215-1229, 2013.
4. Rizvi S and Gores GJ: Molecular pathogenesis of cholangiocarcinoma. Dig Dis 32: 564-569, 2014.
5. Fujiwara M, Kanayama K, Hirokawa YS and Shiraishi T: ASF-4-1 fibroblast-rich culture increases chemoresistance and mTOR expression of pancreatic cancer BxPC-3 cells at the invasive front in vitro, and promotes tumor growth and invasion in vivo. Oncol Lett 11: 2773-2779, 2016.
6. Hasengaowa, Kodama J, Kusumoto T, Shinyo Y, Seki N, Nakamura K, Hongo A and Hiramatsu Y: Loss of basement membrane heparan sulfate expression is associated with tumor progression in endometrial cancer. Eur J Gynaecol Oncol 26: 403-406, 2005.
7. Paduch R: The role of lymphangiogenesis and angiogenesis in tumor metastasis. Cell Oncol (Dordr) 39: 397-410, 2016.
8. Christiansen A and Detmar M: Lymphangiogenesis and cancer. Genes Cancer 2: 1146-1158, 2011.
9. Nakamura Y, Yasuoka H, Tsujimoto M, Imabun S, Nakahara M, Nakao K, Nakamura M, Mori I and Kakudo K: Lymph vessel density correlates with nodal status, VEGF-C expression, and prognosis in breast cancer. Breast Cancer Res Treat 91: 125-132, 2005.
10. Al-Shareef H, Hiraoka SI, Tanaka N, Shogen Y, Lee AD, Bakhshishayan S and Kogo M: Use of NRP1, a novel biomarker, along with VEGF-C, VEGFR-3, CCR7 and SEMA3E, to predict lymph node metastasis in squamous cell carcinoma of the tongue. Oncol Rep 36: 2444-2454, 2016.
11. Schoppmann SF, Berghoff A, Dinhof C, Jakesz R, Gnant M, Dubsky P, Jesch B, Heinzl H and Birner P: Podoplanin-expressing cancer-associated fibroblasts are associated with poor prognosis in invasive breast cancer. Breast Cancer Res Treat 134: 237-244, 2012.
12. Yuan P, Temam S, El-Naggar A, Zhou X, Liu DD, Lee JJ and Mao L: Overexpression of podoplanin in oral cancer and its association with poor clinical outcome. Cancer 107: 563-569, 2006.
13. Takahashi A, Ishii G, Neri S, Yoshida T, Hashimoto H, Suzuki S, Umemura S, Matsumoto S, Yoh K, Niho S, *et al*: Podoplanin-expressing cancer-associated fibroblasts inhibit small cell lung cancer growth. Oncotarget 6: 9531-9541, 2015.
14. Ono S, Ishii G, Nagai K, Takuwa T, Yoshida J, Nishimura M, Hishida T, Aokage K, Fujii S, Ikeda N and Ochiai A: Podoplanin-positive cancer-associated fibroblasts could have prognostic value independent of cancer cell phenotype in stage I lung squamous cell carci: Usefulness of combining analysis of both cancer cell phenotype and cancer-associated fibroblast phenotype. Chest 143: 963-970, 2013.
15. Choi SY, Sung R, Lee SJ, Lee TG, Kim N, Yoon SM, Lee EJ, Chae HB, Youn SJ and Park SM: Podoplanin, α-smooth muscle actin or S100A4 expressing cancer-associated fibroblasts are associated with different prognosis in colorectal cancers. J Korean Med Sci 28: 1293-1301, 2013.
16. Noren NK, Liu BP, Burridge K and Kreft B: p120 catenin regulates the actin cytoskeleton via Rho family GTPases. J Cell Biol 150: 567-580, 2000.
17. Martin-Villar E, Scholl FG, Gamallo C, Yurrita MM, Muñoz-Guerra M, Cruces J and Quintanilla M: Characterization of human PA2.26 antigen (T1alpha-2, podoplanin), a small membrane mucin induced in oral squamous cell carcinomas. Int J Cancer 113: 899-910, 2005.
18. Smith SM and Melrose J: Podoplanin is expressed by a sub-population of human foetal rib and knee joint rudiment chondrocytes. Tissue Cell 43: 39-44, 2011.
19. Ghosh M, Song X, Mouneimne G, Sidani M, Lawrence DS and Condeelis JS: Cofilin promotes actin polymerization and defines the direction of cell motility. Science 304: 743-746, 2004.
20. Chronopoulos A, Robinson B, Sarper M, Cortes E, Auernheimer V, Lachowski D, Attwood S, García R, Ghassemi S, Fabry B, *et al*: ATRA mechanically reprograms pancreatic stellate cells to suppress matrix remodelling and inhibit cancer cell invasion. Nat Commun 7: 12630, 2016.
21. Fukuoka J, Dracheva T, Shih JH, Hewitt SM, Fujii T, Kishor A, Mann F, Shilo K, Franks TJ, Travis WD and Jen J: Desmoglein 3 as a prognostic factor in lung cancer. Hum Pathol 38: 276-283, 2007.
22. Kyzas PA, Geleff S, Batistatou A, Agnantis NJ and Stefanou D: Evidence for lymphangiogenesis and its prognostic implications in head and neck squamous cell carcinoma. J Pathol 206: 170-177, 2005.
23. The National Academies Collection: Reports funded by National Institutes of Health: National Research Council (US) Committee for the Update of the Guide for the Care and Use of Laboratory Animals. Guide for the Care and Use of Laboratory Animals. National Academy of Sciences, 8th edition. Washington (DC), National Academies Press (US), 2011.
24. Wang M, Wu CP, Pan JY, Zheng WW, Cao XJ and Fan GK: Cancer-associated fibroblasts in a human HEp-2 established laryngeal xenografted tumor are not derived from cancer cells through epithelial-mesenchymal transition, phenotypically activated but karyotypically normal. PLoS One 10: e0117405, 2015.
25. Zhou F, Xu Y, Shi J, Lan X, Zou X, Wang L and Huang Q: Expression profile of E-cadherin, estrogen receptors, and P53 in early-onset gastric cancers. Cancer Med 5: 3403-3411, 2016.
26. Gandou C, Harada K, Sato Y, Igarashi S, Sasaki M, Ikeda H and Nakanuma Y: Hilar cholangiocarcinoma and pancreatic ductal adenocarcinoma share similar histopathologies, immunophenotypes, and development-related molecules. Hum Pathol 44: 811-821, 2013.
27. DeOliveira ML, Cunningham SC, Cameron JL, Kamangar F, Winter JM, Lillemoe KD, Choti MA, Yeo CJ and Schulick RD: Cholangiocarcinoma: Thirty-one-year experience with 564 patients at a single institution. Ann Surg 245: 755-762, 2007.

28. Nimura Y, Kamiya J, Kondo S, Nagino M, Uesaka K, Oda K, Sano T, Yamamoto H and Hayakawa N: Aggressive preoperative management and extended surgery for hilar cholangiocarcinoma: Nagoya experience. J Hepatobiliary Pancreat Surg 7: 155-162, 2000.

29. Wicki A and Christofori G: The potential role of podoplanin in tumour invasion. Br J Cancer 96: 1-5, 2007.

30. Pietras K and Ostman A: Hallmarks of cancer: Interactions with the tumor stroma. Exp Cell Res 316: 1324-1331, 2010.

31. Rajaram M, Li J, Egeblad M and Powers RS: System-wide analysis reveals a complex network of tumor-fibroblast interactions involved in tumorigenicity. PLoS Genet 9: e1003789, 2013.

32. Kadota K, Huang CL, Liu D, Nakashima N, Yokomise H, Ueno M and Haba R: The clinical significance of the tumor cell D2-40 immunoreactivity in non-small cell lung cancer. Lung Cancer 70: 88-93, 2010.

33. Chuang WY, Yeh CJ, Wu YC, Chao YK, Liu YH, Tseng CK, Chang HK, Liu HP and Hsueh C: Tumor cell expression of podoplanin correlates with nodal metastasis in esophageal squamous cell carcinoma. Histol Histopathol 24: 1021-1027, 2009.

34. Kalluri R: The biology and function of fibroblasts in cancer. Nat Rev Cancer 16: 582-598, 2016.

35. Navarro A, Perez RE, Rezaiekhaligh M, Mabry SM and Ekekezie II: T1alpha/podoplanin is essential for capillary morphogenesis in lymphatic endothelial cells. Am J Physiol Lung Cell Mol Physiol 295: L543-L551, 2008.

36. Astarita JL, Cremasco V, Fu J, Darnell MC, Peck JR, Nieves-Bonilla JM, Song K, Kondo Y, Woodruff MC, Gogineni A, *et al*: The CLEC-2-podoplanin axis controls the contractility of fibroblastic reticular cells and lymph node micro-architecture. Nat Immunol 16: 75-84, 2015.

37. Collazo J, Zhu B, Larkin S, Martin SK, Pu H, Horbinski C, Koochekpour S and Kyprianou N: Cofilin drives cell-invasive and metastatic responses to TGF-β in prostate cancer. Cancer Res 74: 2362-2373, 2014.

38. Torka R, Thuma F, Herzog V and Kirfel G: ROCK signaling mediates the adoption of different modes of migration and invasion in human mammary epithelial tumor cells. Exp Cell Res 312: 3857-3871, 2006.

39. Ochoa-Alvarez JA, Krishnan H, Pastorino JG, Nevel E, Kephart D, Lee JJ, Retzbach EP, Shen Y, Fatahzadeh M, Baredes S, *et al*: Antibody and lectin target podoplanin to inhibit oral squamous carcinoma cell migration and viability by distinct mechanisms. Oncotarget 6: 9045-9060, 2015.

40. Yoshida T, Ishii G, Goto K, Neri S, Hashimoto H, Yoh K, Niho S, Umemura S, Matsumoto S, Ohmatsu H, *et al*: Podoplanin-positive cancer-associated fibroblasts in the tumor microenvironment induce primary resistance to EGFR-TKIs in lung adenocarcinoma with EGFR mutation. Clin Cancer Res 21: 642-651, 2015.

41. Friedl P and Wolf K: Tumour-cell invasion and migration: Diversity and escape mechanisms. Nat Rev Cancer 3: 362-374, 2003.

42. Zheng X, Carstens JL, Kim J, Scheible M, Kaye J, Sugimoto H, Wu CC, LeBleu VS, and Kalluri R: Epithelial-to-mesenchymal transition is dispensable for metastasis but induces chemoresistance in pancreatic cancer. Nature 527: 525-530, 2015.